SCIENTIFIC REPORTS

OPEN

CONFERENCE PROCEEDINGS

APEnergy2014

SUBJECT AREAS:
POROUS MATERIALS
BATTERIES

Received
28 February 2014

Accepted
22 April 2014

Published
29 August 2014

Correspondence and requests for materials should be addressed to G.X.W. (Guoxiu.Wang@uts.edu.au)

Honeycomb-like porous gel polymer electrolyte membrane for lithium ion batteries with enhanced safety

Jinqiang Zhang, Bing Sun, Xiaodan Huang, Shuangqiang Chen & Guoxiu Wang

Centre for Clean Energy Technology, School of Chemistry and Forensic Science, University of Technology, Sydney, NSW, 2007, Australia.

Lithium ion batteries have shown great potential in applications as power sources for electric vehicles and large-scale energy storage. However, the direct uses of flammable organic liquid electrolyte with commercial separator induce serious safety problems including the risk of fire and explosion. Herein, we report the development of poly(vinylidene difluoride-co-hexafluoropropylene) polymer membranes with multi-sized honeycomb-like porous architectures. The as-prepared polymer electrolyte membranes contain porosity as high as 78%, which leads to the high electrolyte uptake of 86.2 wt%. The PVDF-HFP gel polymer electrolyte membranes exhibited a high ionic conductivity of 1.03 mS cm^{-1} at room temperature, which is much higher than that of commercial polymer membranes. Moreover, the as-obtained gel polymer membranes are also thermally stable up to 350°C and non-combustible in fire (fire-proof). When applied in lithium ion batteries with $LiFePO_4$ as cathode materials, the gel polymer electrolyte demonstrated excellent electrochemical performances. This investigation indicates that PVDF-HFP gel polymer membranes could be potentially applicable for high power lithium ion batteries with the features of high safety, low cost and good performance.

Currently, lithium ion batteries are the dominant power sources for portable electronic devices owing to their high energy density and efficiency. It is also well recognised that lithium batteries are the preferred system for electric vehicles and large-scale energy storage. Despite all efforts to improve the performances of lithium ion batteries, safety concerns remain a formidable challenge, due to the use of flammable liquid organic electrolyte and polymer separator[1,2]. Internal short-circuit and the combustion of the organic electrolyte could cause fire and explosion, which is a major obstacle for large-scale applications of lithium ion batteries.

Solid-state electrolytes can overcome the safety problem of lithium ion batteries because they do not contain flammable liquid chemicals[3–6]. However, solid-state electrolytes based on inorganic Li^+ conductors usually have low ionic conductivity. On the other hand, gel polymer electrolytes, which are prepared by gelling liquid electrolytes with polymer matrices, have advantages over both liquid electrolyte and ceramic (glass) electrolytes. Porous gel polymer electrolytes (PGPEs) combine electrolyte and separator as an integrated membrane[1,2,7–13]. Compared with liquid electrolytes, polymer electrolytes can effectively prevent electrolyte leakage and reduce the firing hazard, which leads to the high safety of batteries. Meanwhile, porous polymer electrolytes can provide high ionic conductivity, good processability, a wide electrochemical operating window, and good thermal stability[14–17]. Especially, several efforts have been made to accomplish polymer electrolyte with enhanced thermal stability towards high temperature[18,19]. The porous structures in polymer membranes are also important because they are responsible for the uptake of liquid electrolytes[2,7]. Though, membranes with too large pores can induce an internal short circuit, causing the failure of batteries. In order to solve this problem, several approaches have been carried out to reduce the pore size, such as embedding inorganic nanoparticles and coating with other polymer matrices[2,7,20–24].

The choices for polymer matrices are versatile. For example, poly(ethylene oxide) (PEO), polyacrylonitrile (PAN), poly(methyl methacrylate) (PMMA), poly(vinylidene fluoride) (PVDF), and poly(vinylidene fluoride-co-hexafluoropropylene) (PVDF-HFP) have been intensively studied[25–31]. Among these polymers, PVDF-HFP has attracted particular interest because its semi-crystallinity, originating from the co-polymerization of amorphous HFP, can trap liquid electrolytes, and crystal VDF can provide mechanical support[32]. Therefore, PVDF-HFP can offer not only high ionic conductivity, but also good mechanical properties. In this paper, PVDF-HFP membranes with honeycomb-like regular porous structures were prepared by a breath-figure method. The as-prepared

PVDF-HFP membranes have a unique porous architecture with highly ordered multi-sized pores. When applied as the separator in lithium ion batteries, PVDF-HFP gel polymer electrolyte membranes exhibited a high ionic conductivity at ambient temperature, an outstanding stability, and fire-proof capability. The as-developed porous gel polymer membranes are attractive for lithium ion batteries with enhanced safety.

Results

Figure 1 shows FESEM images of porous PVDF-HFP gel polymer membranes. The membrane peeled from the glass substrate has two different sides. For convenience, the side in direct contact with humid air is defined as the front side, and the other side in direct contact with the glass substrate is called the back side. In Figure 1(a), an ordered honeycomb-like structure can be observed on the front side of the membrane. The diameters of the regular pores are in the range of 2 to 3 μm. The high magnification SEM image shown in Figure 1(b) indicates that there are also smaller pores inside the regular pores on the front surface of the membrane. This unique hierarchical porous structure could provide high porosity for further absorption of electrolyte. However, on the back side of the membrane, much less density of pores can be observed (as shown in Figure 1(c) and 1(d)). The diameters of the pores are smaller than 1 μm. Although the size and amount of the pores have decreased, these pores still interconnect inside the membrane (as shown in Figure 1(d)), which can provide a path way for fast ion transportation. Figure 1(e) and 1(f) show the FESEM images of the cross-section of the membrane. The thickness of the PVDF-HFP membrane is around 8 to 10 μm, which is thinner than the separators obtained by other techniques[1,2,7]. It is very interesting to find that the porosity, diameters and regularity of pores decrease from the front side to the back side of the membrane. The three-dimension structure of the front side is shown in Figure 1(e) and the structure of the back side is shown in Figure 1(f). These results are consistent with the observation shown in Figure 1(a) ~ (d) and Figure S1 (Electronic Supplementary Information, ESI). The low porosity on the back side can prevent the risk of short circuit when applied in lithium ion batteries.

The formation of this unique porous structure could originate from the breath-figure preparation method[33–39]. The preparation process is illustrated in Figure 2(a). When PVDF-HFP/acetone solution is naturally evaporated in an atmosphere with high humidity, water droplets will deposit onto the surface of the solution because of the decrease of the local temperature, owing to the endothermic nature of the evaporating process. PVDF-HFP molecules will gather and create a polymer shield around the water droplets. The water

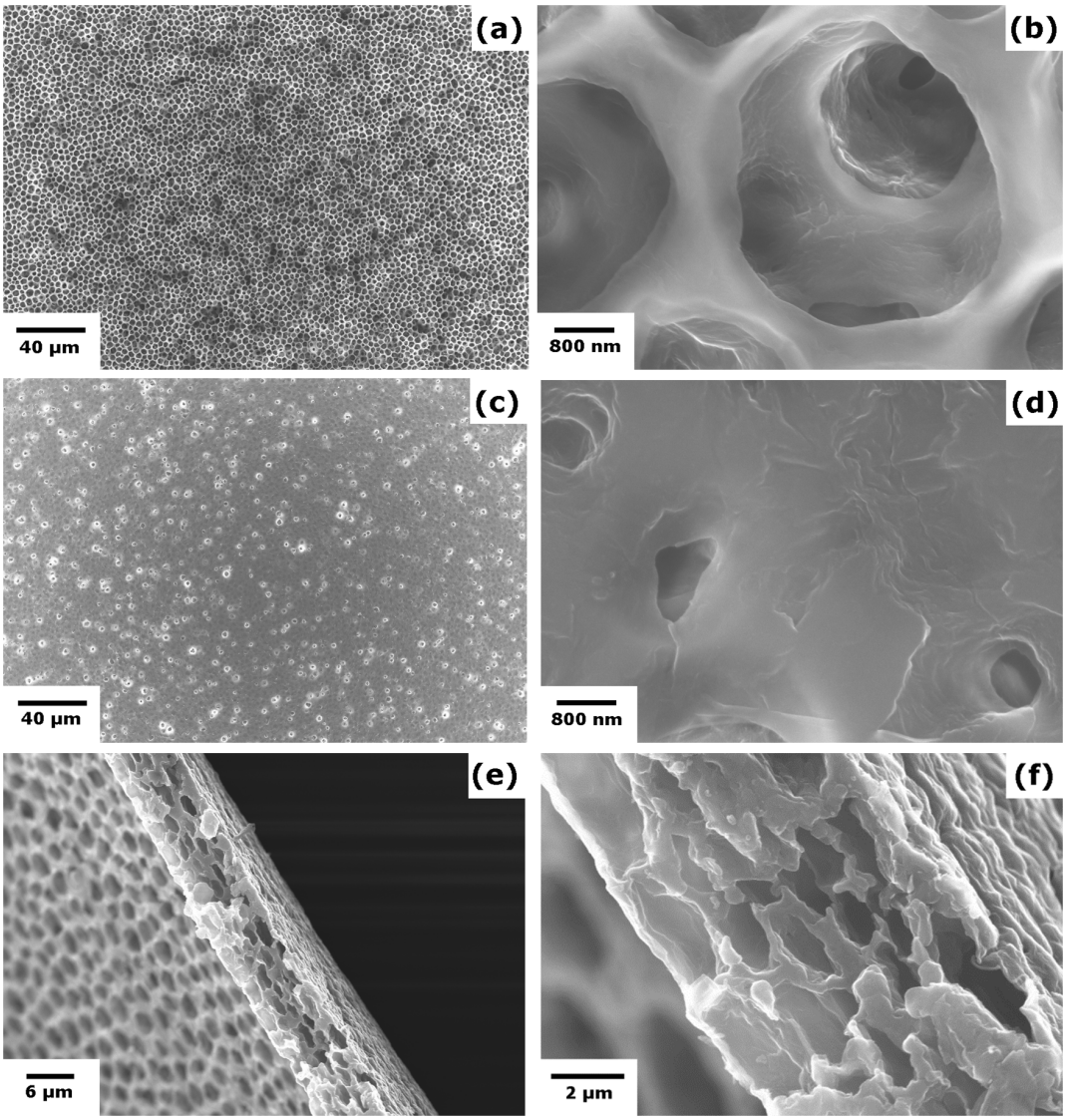

Figure 1 | FESEM images of (a, b) the front side, (c, d) the back side, and (e, f) the cross-section of the PVDF-HFP honeycomb-like porous polymer membrane.

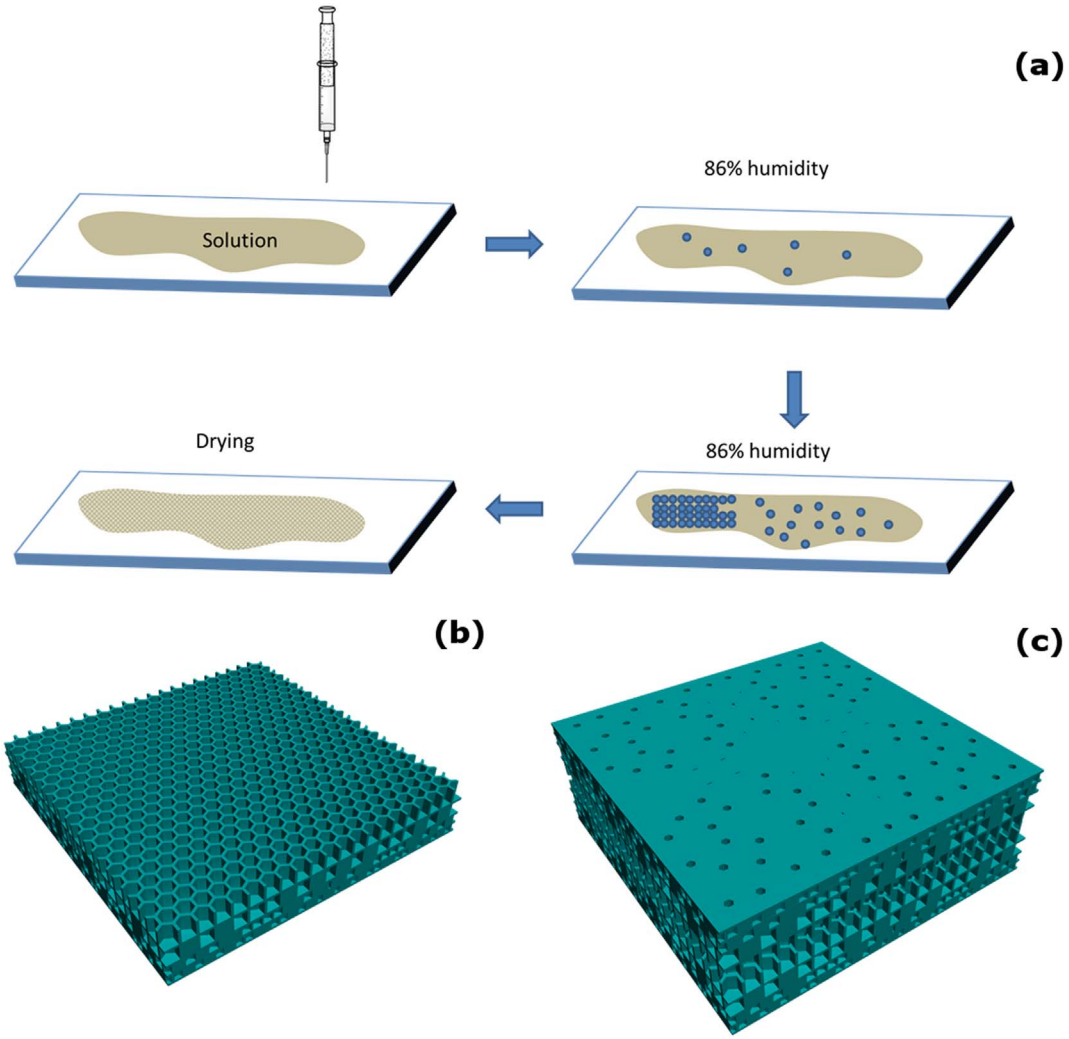

Figure 2 | Schematic illustration: (a) The preparation process of the PVDF-HFP porous polymer membrane. (b) The 3D architecture of PVDF-HFP polymer membrane. And (c) the porous gel polymer electrolyte with the combination of two membranes as one integrated separator (two back sides are exposed to the outside).

droplets will then further re-assemble and pack into a regular hexagonal pattern owing to the capillary force on the solution surface, which leads to the formation of the honeycomb-like architecture. After the formation of the first layer, the water droplets in the second layer are not facile to assemble into a regular porous structure because of the geometry blocking effect from the first layer and the decrease of humidity. This induces lower regularity, smaller size of pores and lower porosity. On the bottom of the membrane, the humidity is very low and the morphology is also influenced by the flat surface of the glass substrate, which results in a flat morphology with lower porosity and smaller pore size than that on the front side of the membrane. Figure 2(b) shows the schematic structure of the obtained PVDF-HFP porous membrane, which is consistent with the SEM images shown in Figure 1.

In order to make better usage of the unique multi-porous architecture, we combined two membranes to make one separator. The honeycomb-like front side was put inside together with the back side exposed to the outside (as shown in Figure 2(c)). The thickness of the double-layered membrane is similar to the separators. The large, highly ordered pores inside the membranes are responsible for the absorption of electrolyte, while the flat back side exposed to the outside could help obstruct the transportation of electrode particles and the growth of lithium dendrite during cell operation. All the pores are interconnected and provide pathways for fast lithium ion transport. This unique double-layered membrane is expected to deliver good electrochemical performance when applied in lithium ion batteries.

Figure S2 (ESI) shows the FTIR spectrum of the PVDF-HFP membrane. The characteristic peaks of PVDF-HFP copolymer are clearly presented in the spectrum. The peaks at 3028 and 2977 cm^{-1} originate from the stretching of -CH_2- group and the peak at 1651 cm^{-1} is assigned to the –CH=CF- skeletal bending. The –C-F stretching peak is shown at 1401 cm^{-1}. The broad peaks near 1187 cm^{-1} are from the stretching of –CF_2-. The other peaks at 1065 (C-C skeletal vibration), 877 (vinylidene group), 841 (-CH_2- rocking), 757 (-CF_3 stretching), 669 (-CH_2- bending), 601 (-CF_2- bending) and 489 cm^{-1} (-CF_2- wagging) are all characteristic peaks of PVDF-HFP copolymer.

The stability of polymer electrolyte at high temperature is very crucial for Li-ion battery application. Figure 3 shows the thermogravimetry (TG) and differential scanning calorimetry (DSC) curves of the PVDF-HFP membrane. As shown in Figure 3, the membrane is thermally stable up to 140°C and only shows a slight decrease in weight up to 350°C, which is consistent with the DSC curve shown in Figure 3. There is an endothermic peak at 140°C, which probably is related to the melting point of the PVDF-HFP. When the temperature increases above 150°C, the membrane does not show endothermic peaks in air atmosphere. This indicates that the PVDF-HFP

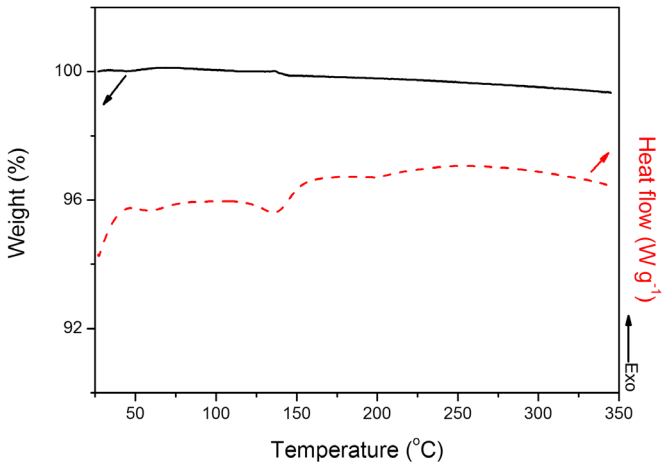

Figure 3 | Thermogravimetry (TG, solid line) and differential scanning calorimetry (DSC, dot line) curves of PVDF-HFP porous polymer membrane in air. The temperature rising rate is 10°C min^{-1}.

membrane is stable in the air at high temperature. The conventional separators usually shrink when the temperature reaches or exceeds the melting point, which causes an internal short circuit. In order to further investigate the dimensional stability of PVDF-HFP membranes in high temperature, the membrane was stored at 150°C for 30 min. Figure 4(a) and (b) show the digital photos of the membrane before and after heating. The PVDF-HFP membrane maintained the dimensional stability. This unique thermal property can effectively prevent the potential short circuit in lithium ion batteries. Conventional separators easily catch fire, and cause an explosion. Since PVDF-HFP is fire-resistant, PVDF-HFP polymer membranes should be fire-proof. Figure 4(c) and (d) show the digital photos of the membrane before and after being set on fire. Obviously, PVDF-HFP membranes can resist fire. The high thermal stability of the PVDF-HFP polymer membrane is desirable for lithium power batteries.

The electrolyte retention capability of the PVDF-HFP polymer membrane was evaluated by TG and DSC analyses. Figure S3 (ESI) shows the TG and DSC curves of the polymer membrane saturated with organic liquid electrolyte. The weight of the polymer membrane gradually decreases before 60°C, which is probably related to the evaporation of electrolyte on the surface of the membrane. When the temperature increases to 150°C, the polymer membrane with organic liquid electrolyte shows 40% weight loss, which is from the evaporation of the liquid electrolyte. However, compared with 86.2% electrolyte uptake calculated by measuring the mass before and after absorption, the content of retained electrolyte in the porous polymer membrane is still very high and sufficient for electrochemical characterization when heating to 150°C. Such good electrolyte retention capability can ensure the lithium ion battery operation at elevated temperatures.

Ionic conductivity of the polymer electrolyte is the most critical factor in achieving good electrochemical performance of lithium ion batteries. Figure 5 shows the ionic conductivity dependence on temperatures of the PVDF-HFP polymer membrane and Celgard 2400 separator in the range of 25°C to 65°C. The ionic conductivities were calculated from the a.c. impedance plots shown in the inset in Figure 5. The resistance of the bulk electrolyte was obtained from the intercept of the straight line on the real axis. The ionic conductivity of the PVDF-HFP polymer electrolyte membrane is 1.03 mS cm^{-1} at room temperature which is higher than the Celgard 2400 separator saturated with electrolyte (0.60 mS cm^{-1}), and increases with a rising temperature[40,41]. Such high ionic conductivity should be ascribed to the high porosity of the polymer membrane. There are three phases in the PVDF-HFP polymer electrolyte membrane, including solid polymer matrix, swollen polymer and absorbed liquid electrolyte solution. It is well known that polymer matrix is the mechanical support of the polymer electrolyte, while the absorbed liquid electrolyte solution is responsible for ionic conductivity. The PVDF-HFP polymer membrane has a porosity as high as 78%, which leads to high percentage electrolyte uptake (86.2 wt%). The pores in the membrane are also interconnected with each other, which is a further benefit for delivering high ionic conductivity.

The dependence of the ionic conductivity on temperature can be evaluated by the Arrhenius Equation,

$$\sigma = A\ \exp(-E_a/RT) \quad (1)$$

where A is the pre-exponential factor and E_a is activation energy. The calculated E_a value is 12.05 kJ mol^{-1}. This value is very similar to the activation energy of liquid electrolyte in Celgard 2400 separator (11.12 kJ mol^{-1}). This further explains the high ionic conductivity.

Discussion

The electrochemical stability of the PVDF-HFP polymer electrolyte membrane was assessed by assembling Li-ion typed cells with the

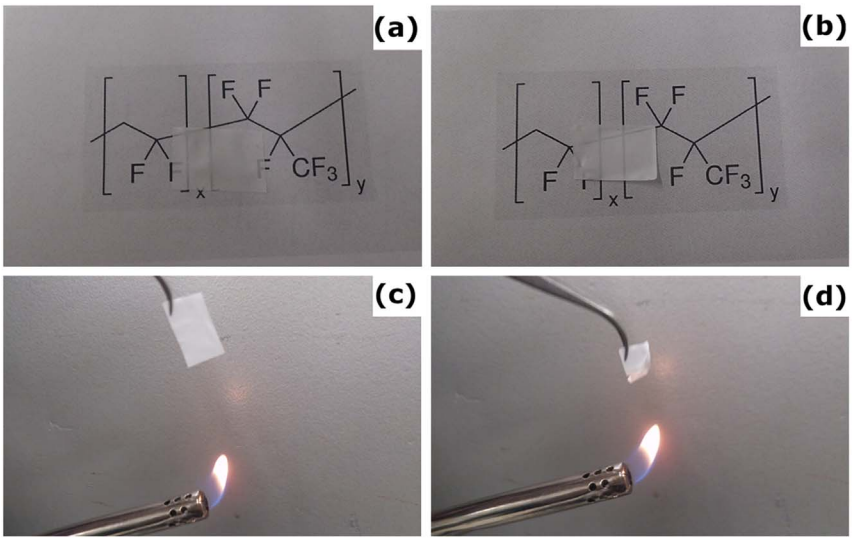

Figure 4 | The thermal shrinking test of the PVDF-HFP porous membrane (a) before and (b) after heating to 150°C for 30 min, and the combustion test of the membrane (c) before and (d) after set on fire.

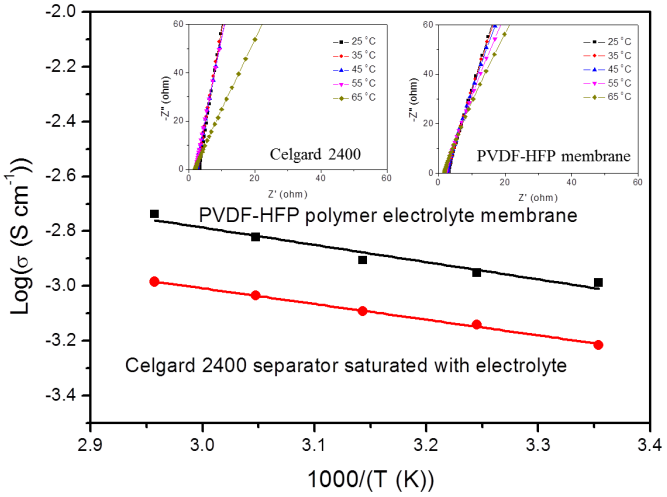

Figure 5 | **The Arrhenius plots of the ionic conductivity vs. temperature.** The inset is the a.c. impedance spectra.

polymer electrolyte membrane sandwiched between a lithium metal electrode and stainless steel electrode. As shown in Figure S4 (ESI), there is no obvious reaction peak up to 5 V, which indicates that the polymer electrolyte is stable up to 5 V. Normally, a stability window of up to 4.5 V is sufficient for the operation of lithium ion batteries[42].

The electrochemical performances of the lithium ion battery with PVDF-HFP polymer electrolyte were further tested in coin type cells. Figure S5 (ESI) shows the cyclic voltammetry curve of the assembled lithium ion cells. The redox potentials are 3.2 V and 3.6 V respectively, corresponding to the intercalation and de-intercalation of Li^+ in $LiFePO_4$ electrodes[43]. Figure 6 shows the electrochemical performances of lithium ion cells with $LiFePO_4$ as cathode materials, using PVDF-HFP polymer electrolyte membrane and Celgard 2400 as separators. The cut-off voltage was set at 2 V for discharge and 4.2 V for charge. Figure 6(a) shows the typical charge-discharge curves of the assembled lithium ion cells with PVDF-HFP polymer electrolyte membranes at the current density of 0.2 C (1 C = 170 mA g^{-1}). The charge and discharge plateaus are both around 3.4 V and the voltage difference between charge and discharge curves is smaller than 0.1 V, which is very similar to the direct use of liquid electrolyte with commercial separator (as shown in Figure 6(b))[44–47]. The small over-potential maintains after 50 cycles, which suggests the capability of PVDF-HFP polymer electrolyte membranes to support superior battery performances. Figure 6(c) shows the cycling performances of lithium ion batteries with PVDF-HFP polymer electrolyte and liquid electrolyte. The lithium ion battery with PVDF-HFP polymer electrolyte could operate at least 50 cycles with no

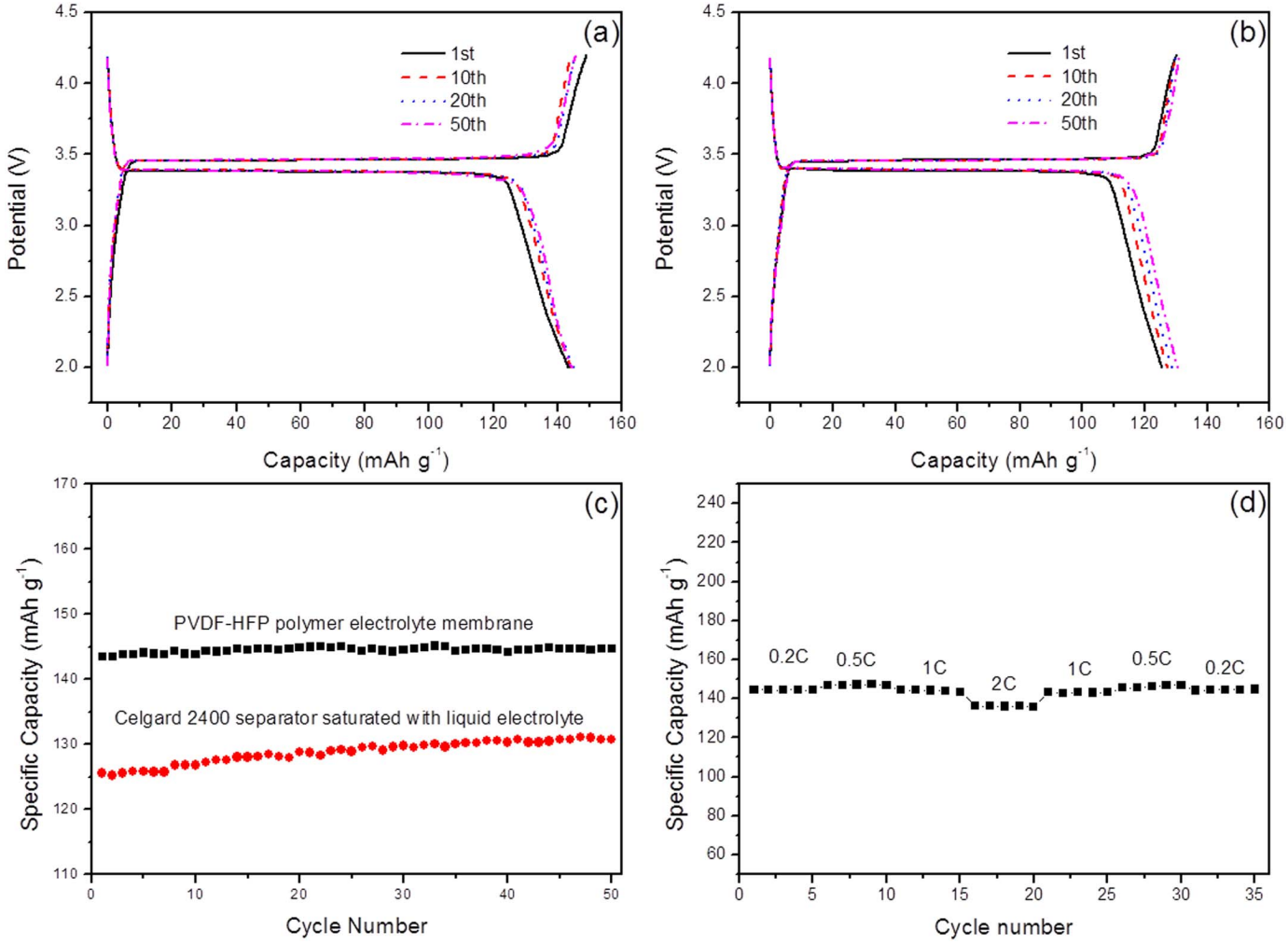

Figure 6 | Electrochemical performances of lithium ion cells with $LiFePO_4$ as cathode materials: (a) Charge-discharge curves using PVDF-HFP polymer electrolyte membranes, (b) Charge-discharge curves using Celgard 2400 separators saturated with liquid electrolyte, (c) Cycling performances. The cut-off voltages are 2 V and 4.2 V. The current density is 0.2 C. (d) Rate behaviour. The current densities of discharge and charge are 0.2 C, 0.5 C, 1 C, and 2 C respectively.

obvious capacity degradation. The reversible capacity of the lithium ion battery with PVDF-HFP polymer electrolyte was about 145 mAh g^{-1} at 0.2 C, which is higher than that with a Celgard 2400 separator (130 mAh g^{-1}). The discharge performance of the lithium ion battery with PVDF-HFP polymer electrolyte at 1 C also showed good cycling stability up to 100 cycles (Figure S6, ESI). When the cells were operated under different current densities, the capacity slightly decreased with the increase of the current density from 0.5 C to 2 C (as shown in Figure 6(d)). When the current density decreased back to 0.2 C, the reversible capacity recovered to its original value. The discharge and charge curves, shown in Figure S7 (ESI), indicate the over-potential did not significantly increase when the current density escalated. These results further illustrate the PVDF-HFP polymer electrolyte membranes can support outstanding rate performances. Such high performances of lithium ion battery with PVDF-HFP polymer electrolyte are related to the multi-sized porous architecture of the PVDF-HFP polymer membrane. The large and interconnected pores inside the membrane provide high ionic conductivity, and the outside flat surface prevents lithium dendrite growth and short circuiting, which eliminates the safety concerns and ensures a long and sufficient cycle life of lithium ion batteries.

Methods

Preparation of PVDF-HFP polymer electrolyte membranes. PVDF-HFP based porous membranes were prepared by a breath-figure method[33,34]. In the first step, PVDF-HFP (Sigma-Aldrich, Mw = 455,000) was dissolved in acetone solvent by mechanical stirring to obtain a homogeneous 10% PVDF-HFP/acetone solution. Then the solution was casted onto a flat glass substrate and allowed to dry under a controlled humidity of 86%. After fully drying, the obtained membrane was peeled off from the substrate and dried again in a vacuum oven at 60°C for 12 h. The polymer electrolyte membranes were prepared by immersing the porous membrane overnight into 1 M $LiPF_6$ in 1 : 1 ethylene carbonate (EC): dimethyl carbonate (DMC) liquid electrolyte. The excess liquid residue on the membrane surface was carefully wiped off with a tissue.

Characterization of PVDF-HFP membranes. A field emission scanning electron microscope (FESEM, Zeiss Supra 55 VP) was used to investigate the morphology of the as-prepared PVDF-HFP porous membrane. Thermal stability of the polymer membrane was measured by Thermogravimetric analysis using a Mettle Toledo TGA/DSC instrument. Infrared spectroscopy was conducted on a Nicolet Magna 6700 FT-IR spectrometer. All spectra were obtained using 4 cm^{-1} resolution and 64 scans at room temperature.

The porosity of the polymer membrane was measured using *n*-butanol. The membrane was immersed in *n*-butanol for 2 h. The porosity of the polymer membranes was calculated based on the Equation 2.

$$p = \frac{(m_a - m_p)/\rho_a}{(m_a - m_p)/\rho_a + m_p/\rho_p} \quad (2)$$

where p is the porosity, m_a and m_p are the mass of the membrane after and before the absorption of *n*-butanol, respectively, while ρ_a and ρ_p are the density of *n*-butanol and the polymer matrix, respectively.

The amount of liquid electrolyte uptake is calculated using the Equation 3.

$$\eta = \frac{W_t - W_o}{W_o} \times 100\% \quad (3)$$

where η is the uptake of liquid electrolyte, and W_o and W_t are the weights of the membranes before and after absorption of liquid electrolyte respectively.

Electrochemical characterization of PVDF-HFP electrolyte membrane. Linear sweep voltammetry measurements were conducted to determine the stability of the PVDF-HFP polymer membrane. The polymer membrane was sandwiched between a lithium anode and stainless steel (SS) electrode. The electrochemical impedances at different temperatures were measured by sandwiching polymer electrolyte membranes between two stainless steel electrodes. The ionic conductivity was calculated using the Equation 4.

$$\sigma = d/(R_b \times S) \quad (4)$$

where σ is the ionic conductivity, d is the thickness of the PGPE, R_b is the bulk resistance, and S is the area of the electrodes. All these electrochemical characterizations were conducted using a CH Instrument 660D electrochemical workstation.

The electrochemical performances of Li-ion batteries with PVDF-HFP polymer membrane was conducted by assembling CR2032 coin cells with lithium metal as the counter and reference electrode. $LiFePO_4$ prepared by conventional solid state reaction was used as the working electrode active material. The working electrode was prepared by first mixing PVDF (10%), carbon black (10%), and $LiFePO_4$ (80%) together in 1-Methyl-2-pyrrolidinone (NMP, Sigma-Aldrich). The mixture was then coated onto aluminium foil, dried at 80°C for 12 h under vacuum, and punched into disks. All cells were assembled in an argon-filled glove box with water and oxygen content lower than 0.1 ppm.

1. Zhu, Y. S. *et al.* A single-ion polymer electrolyte based on boronate for lithium ion batteries. *Electrochem. Commun.* **22**, 29–32 (2012).
2. Zhu, Y. *et al.* Composite of a nonwoven fabric with poly(vinylidene fluoride) as a gel membrane of high safety for lithium ion battery. *Energy Environ. Sci.* **6**, 618–624 (2013).
3. Christie, A. M., Lilley, S. J., Staunton, E., Andreev, Y. G. & Bruce, P. G. Increasing the conductivity of crystalline polymer electrolytes. *Nature* **433**, 50–53 (2005).
4. MacGlashan, G. S., Andreev, Y. G. & Bruce, P. G. Structure of the polymer electrolyte poly(ethylene oxide)(6): LiAsF6. *Nature* **398**, 792–794 (1999).
5. Varshney, P. K. & Gupta, S. Natural polymer-based electrolytes for electrochemical devices: a review. *Ionics* **17**, 479–483 (2011).
6. Croce, F., Appetecchi, G. B., Persi, L. & Scrosati, B. Nanocomposite polymer electrolytes for lithium batteries. *Nature* **394**, 456–458 (1998).
7. Kim, M. & Park, J. H. Multi-Scale Pore Generation from Controlled Phase Inversion: Application to Separators for Li-Ion Batteries. *Adv. Energy Mater.* **3**, 1417–1420 (2013).
8. Abraham, K. M., Jiang, Z. & Carroll, B. Highly conductive PEO-like polymer electrolytes. *Chem. Mater.* **9**, 1978–1988 (1997).
9. Meyer, W. H. Polymer electrolytes for lithium-ion batteries. *Adv. Mater.* **10**, 439–+ (1998).
10. Song, J. Y., Wang, Y. Y. & Wan, C. C. Review of gel-type polymer electrolytes for lithium-ion batteries. *J. Power Sources* **77**, 183–197 (1999).
11. Arora, P. & Zhang, Z. M. Battery separators. *Chem. Rev.* **104**, 4419–4462 (2004).
12. Zhang, S. S. A review on the separators of liquid electrolyte Li-ion batteries. *J. Power Sources* **164**, 351–364 (2007).
13. Li, Z. H., Su, G. Y., Wang, X. Y. & Gao, D. S. Micro-porous P(VDF-HFP)-based polymer electrolyte filled with Al2O3 nanoparticles. *Solid State Ionics* **176**, 1903–1908 (2005).
14. Shi, Q., Yu, M. X., Zhou, X., Yan, Y. S. & Wan, C. R. Structure and performance of porous polymer electrolytes based on P(VDF-HFP) for lithium ion batteries. *J. Power Sources* **103**, 286–292 (2002).
15. Magistris, A., Quartarone, E., Mustarelli, P., Saito, Y. & Kataoka, H. PVDF-based porous polymer electrolytes for lithium batteries. *Solid State Ionics* **152**, 347–354 (2002).
16. Song, J. M., Kang, H. R., Kim, S. W., Lee, W. M. & Kim, H. T. Electrochemical characteristics of phase-separated polymer electrolyte based on poly(vinylidene and ethylene fluoride-co-hexafluoropropane) carbonate. *Electrochim. Acta* **48**, 1339–1346 (2003).
17. Sundaram, N. T. K. & Subramania, A. Microstructure of PVdF-co-HFP based electrolyte prepared by preferential polymer dissolution process. *J. Membr. Sci.* **289**, 1–6 (2007).
18. Li, Y.-H. *et al.* A novel polymer electrolyte with improved high-temperature-tolerance up to 170 degrees C for high-temperature lithium-ion batteries. *J. Power Sources* **244**, 234–239 (2013).
19. Wu, X.-L. *et al.* Enhanced working temperature of PEO-based polymer electrolyte via porous PTFE film as an efficient heat resister. *Solid State Ionics* **245**, 1–7 (2013).
20. Augustin, S., Hennige, V., Horpel, G. & Hying, C. Ceramic but flexible: new ceramic membrane foils for fuel cells and batteries. *Desalination* **146**, 23–28 (2002).
21. Kim, M., Sohn, J. Y., Nho, Y. C. & Park, J. H. Effects of E-beam Irradiation on Physical and Electrochemical Properties of Inorganic Nanoparticle Separators with Different Particle Sizes. *J. Electrochem. Soc.* **158**, A511–A515 (2011).
22. Jeong, H.-S., Kim, J. H. & Lee, S.-Y. A novel poly(vinylidene fluoride-hexafluoropropylene)/poly(ethylene terephthalate) composite nonwoven separator with phase inversion-controlled microporous structure for a lithium-ion battery. *J. Mater. Chem.* **20**, 9180–9186 (2010).
23. Jeong, H.-S., Choi, E.-S., Kim, J. H. & Lee, S.-Y. Potential application of microporous structured poly(vinylidene fluoride-hexafluoropropylene)/poly(ethylene terephthalate) composite nonwoven separators to high-voltage and high-power lithium-ion batteries. *Electrochim. Acta* **56**, 5201–5204 (2011).
24. Zhang, H. P. *et al.* A novel sandwiched membrane as polymer electrolyte for lithium ion battery. *Electrochem. Commun.* **9**, 1700–1703 (2007).
25. Gentili, V., Panero, S., Reale, P. & Scrosati, B. Composite gel-type polymer electrolytes for advanced, rechargeable lithium batteries. *J. Power Sources* **170**, 185–190 (2007).
26. Raghavan, P. *et al.* Electrochemical performance of electrospun poly(vinylidene fluoride-co-hexafluoropropylene)-based nanocomposite polymer electrolytes incorporating ceramic fillers and room temperature ionic liquid. *Electrochim. Acta* **55**, 1347–1354 (2010).
27. Wang, Y.-J. & Kim, D. Crystallinity, morphology, mechanical properties and conductivity study of in situ formed PVdF/LiClO4/TiO2 nanocomposite polymer electrolytes. *Electrochim. Acta* **52**, 3181–3189 (2007).

28. Pu, W. H., He, X. M., Wang, L., Jiang, C. Y. & Wan, C. R. Preparation of PVDF-HFP microporous membrane for Li-ion batteries by phase inversion. *J. Membr. Sci.* **272**, 11–14 (2006).
29. Zhao, Y.-H., Xu, Y.-Y. & Zhu, B.-K. Effect of amphiphilic hyperbranched-star polymer on the structure and properties of PVDF based porous polymer electrolytes. *Solid State Ionics* **180**, 1517–1524 (2009).
30. Li, Z. H. *et al.* Effects of the porous structure on conductivity of nanocomposite polymer electrolyte for lithium ion batteries. *J. Membr. Sci.* **322**, 416–422 (2008).
31. Miao, R. *et al.* PVDF-HFP-based porous polymer electrolyte membranes for lithium-ion batteries. *J. Power Sources* **184**, 420–426 (2008).
32. Stephan, A. M. & Nahm, K. S. Review on composite polymer electrolytes for lithium batteries. *Polymer* **47**, 5952–5964 (2006).
33. Heng, L., Wang, B., Li, M., Zhang, Y. & Jiang, L. Advances in Fabrication Materials of Honeycomb Structure Films by the Breath-Figure Method. *Materials* **6**, 460–482 (2013).
34. Widawski, G., Rawiso, M. & Francois, B. SELF-ORGANIZED HONEYCOMB MORPHOLOGY OF STAR-POLYMER POLYSTYRENE FILMS. *Nature* **369**, 387–389 (1994).
35. Srinivasarao, M., Collings, D., Philips, A. & Patel, S. Three-dimensionally ordered array of air bubbles in a polymer film. *Science* **292**, 79–83 (2001).
36. Bolognesi, A. *et al.* Self-organization of polystyrenes into ordered microstructured films and their replication by soft lithography. *Langmuir* **21**, 3480–3485 (2005).
37. Li, M. Q., Xu, S. Q. & Kumacheva, E. Convection in polymeric fluids subjected to vertical temperature gradients. *Macromolecules* **33**, 4972–4978 (2000).
38. Peng, J., Han, Y. C., Fu, J., Yang, Y. M. & Li, B. Y. Formation of regular hole pattern in polymer films. *Macromol. Chem. Phys.* **204**, 125–130 (2003).
39. Dimitrov, A. S. & Nagayama, K. Continuous convective assembling of fine particles into two-dimensional arrays on solid surfaces. *Langmuir* **12**, 1303–1311 (1996).
40. Li, Z. H., Cheng, C., Zhan, X. Y., Wu, Y. P. & Zhou, X. D. A foaming process to prepare porous polymer membrane for lithium ion batteries. *Electrochim. Acta* **54**, 4403–4407 (2009).
41. Zhang, P. *et al.* Enhanced electrochemical and mechanical properties of P(VDF-HFP)-based composite polymer electrolytes with SiO2 nanowires. *J. Membr. Sci.* **379**, 80–85 (2011).
42. Xu, J. J. & Ye, H. Polymer gel electrolytes based on oligomeric polyether/cross-linked PMMA blends prepared via in situ polymerization. *Electrochem. Commun.* **7**, 829–835 (2005).
43. Yu, D. Y. W. *et al.* Study of LiFePO4 by cyclic voltammetry. *J. Electrochem. Soc.* **154**, A253–A257 (2007).
44. Yamada, A. *et al.* Room-temperature miscibility gap in Li(x)FePO(4). *Nat. Mater.* **5**, 357–360 (2006).
45. Liu, H. *et al.* Doping effects of zinc on LiFePO4 cathode material for lithium ion batteries. *Electrochem. Commun.* **8**, 1553–1557 (2006).
46. Liu, J., Conry, T. E., Song, X., Doeff, M. M. & Richardson, T. J. Nanoporous spherical LiFePO4 for high performance cathodes. *Energy Environ. Sci.* **4**, 885–888 (2011).
47. Sun, C., Rajasekhara, S., Goodenough, J. B. & Zhou, F. Monodisperse Porous LiFePO4 Microspheres for a High Power Li-Ion Battery Cathode. *J. Am. Chem. Soc.* **133**, 2132–2135 (2011).

Acknowledgments

This original research was proudly supported by Commonwealth of Australia through the Automotive Australia 2020 Cooperative Research Centre (AutoCRC).

Author contributions

G.W. proposed the conceptual idea, participated in writing the manuscript. J.Z. performed the major part of the experiments, organised the data, and wrote the manuscript. B.S. prepared the cathodes and involved in experiments, discussion. X.H. involved in discussion. S.C. involved in processing the data. All authors read and approved the final manuscript.

Additional information

Supplementary information accompanies this paper at http://www.nature.com/scientificreports

Competing financial interests: The authors declare no competing financial interests.

How to cite this article: Zhang, J., Sun, B., Huang, X., Chen, S. & Wang, G. Honeycomb-like porous gel polymer electrolyte membrane for lithium ion batteries with enhanced safety. *Sci. Rep.* **4**, 6007; DOI:10.1038/srep06007 (2014).